JOURNAL OF CATALYSIS 110, 1–10 (1988)

An Interpretation of the High-Pressure Kinetics of Ammonia Synthesis Based on a Microscopic Model

P. STOLTZE* AND J. K. NØRSKOV*,†

* *Haldor Topsøe Research Laboratories, DK-2800 Lyngby, Denmark; and* †*NORDITA, DK-2100 Copenhagen Ø, Denmark*

Received August 27, 1986; revised April 27, 1987

The kinetics of ammonia synthesis at high pressures have been investigated using a recent microscopic model (P. Stoltze and J. K. Nørskov, *Phys. Rev. Lett.* **55**, 2502 (1985)). The model is based on the picture of catalysis emerging from quantum mechanical calculations and the results of available ultrahigh-vacuum single-crystal studies of Fe. No reference to measurements of catalytic reaction rates is used in the determination of the input parameters. The model predicts reaction rates in agreement with experiments using the industrial catalyst over large intervals of reaction conditions. This strongly suggests that the model reproduces the essential features of the kinetics of ammonia synthesis. From the model it is found that the largest contribution to the activation enthalpy for the catalytic synthesis of NH_3 at high pressures is the energetic cost of creating two free sites on the surface of the working catalyst. The calculated activation enthalpy under typical high-pressure reaction conditions is almost but not completely constant. The predicted values are in good agreement with experiment. It is shown that the reaction orders for N_2, H_2, and NH_3 are directly related to the surface coverages by reaction intermediates. The calculated reaction orders at high pressures are in good agreement with those observed in many previous investigations. The coverages by adsorbed NH, NH_2, NH_3, and H species are found to be larger than the "coverage by free sites," i.e., the fraction of unoccupied sites. We suggest that this is the reason why the kinetics of ammonia synthesis cannot be well described by a Langmuir–Hinshelwood expression with only one surface intermediate. It is further shown that the observed high-pressure kinetics may be explained without the assumption of surface heterogeneity used in the usual derivation of the Temkin–Pyzhev or Ozaki–Taylor–Boudart kinetics.

1. INTRODUCTION

In recent years a number of chemisorption processes of importance for industrial catalysis have been investigated in detail (*1–11*) using surface-science techniques and well-defined single-crystal surfaces. The theoretical description of chemisorption has also developed considerably (*12–21*). This has resulted in an identification of some of the parameters underlying poisoning and promotion (*12, 21*) and trends in reactivities for the transition metals as catalysts (*12, 21*).

Direct measurements of rates of catalytic reactions have been made for single crystals as catalysts at high pressures (*4, 8, 22–25*) and found to be in agreement with rates measured for polycrystalline, supported metals for methanation over Ni (*2, 8, 22*), for CO oxidation over Rh (*25*), and for ammonia synthesis over Fe (*22, 23, 26*).

An attempt to use the available results of UHV single-crystal studies to formulate a model of ammonia synthesis was made by Bowker *et al.* (*27*). They calculated rates of ammonia synthesis which were too low by a factor of 10^5 and concluded on this basis that the reaction mechanism should be different at low and high pressures. We ascribe the discrepancy between experiment and the calculations by these authors to an inconsistency in their description of the adsorption and desorption of N_2 (*28, 29*).

Boudart and Löffler have noted (*26*) that the high-pressure catalytic rates measured for ammonia synthesis over single crystals (*22, 23*) are in agreement with measure-

0021-9517/88 $3.00

ments for supported, polycrystalline Fe (*60*). This suggests that studies of ammonia synthesis over Fe single crystals are directly applicable to the study of ammonia synthesis over polycrystalline Fe.

We have developed a model (*28*) for ammonia synthesis based on quantum mechanical calculations (*12, 13, 15, 19, 21*) and UHV single-crystal studies (*1–3, 9, 11, 22, 23, 30–35*) of the adsorption of N_2, H_2, and NH_3 on Fe and on K-precovered Fe. The model contains no adjustable parameters and predicts rates of ammonia synthesis in quite good agreement with high-pressure measurements using an industrial catalyst. This is a demonstration that the "pressure gap" between UHV single-crystal studies and high pressure catalysis can be bridged.

The purpose of our model is to formulate a framework for the understanding of the high-pressure synthesis of ammonia using a physically simple model. The purpose is not to obtain a high accuracy in predictions of catalytic reaction rates or to be able to resolve the kinetics in the finest details. The initial test of the model is the comparison of experimental and predicted reaction rates (*28*). The ultimate test of the model will be its usefulness in the interpretation of single-crystal experiments and of high-pressure reaction measurements. We demonstrate here how our model can be used in an interpretation of the observed high-pressure kinetics of ammonia synthesis.

2. THE MODEL OF THE ACTIVE CATALYST

The industrial ammonia synthesis catalyst consists of Fe promoted with small amounts of K, Al, and Ca (*36–38*). In the active state of the catalyst Fe is present as 200- to 500-Å crystallites of the metal (*39, 40*). Al and Ca are present as oxides in the surface (*41*) of the Fe crystallites and serve to increase and stabilize the dispersion of Fe (*39, 42–45*). K is present on the Fe surface (*42*) and increases the catalyst activity by increasing the turnover frequency for each site (*1–3, 9, 11–13, 19, 21, 46, 47*).

3. THE REACTION MECHANISM

By kinetic studies on the catalyst (*37, 48–51*) and by the study of N_2 adsorption on single crystals of Fe (*1, 2, 9, 11, 21*), the following reaction scheme has been established,

$$N_2\,(g) + * = N_2\text{-}* \quad (1)$$

$$N_2\text{-}* + * = 2N\text{-}* \quad (2)$$

$$N\text{-}* + H\text{-}* = NH\text{-}* + * \quad (3)$$

$$NH\text{-}* + H\text{-}* = NH_2\text{-}* + * \quad (4)$$

$$NH_2\text{-}* + H\text{-}* = NH_3\text{-}* + * \quad (5)$$

$$NH_3\text{-}* = NH_3\,(g) + * \quad (6)$$

$$H_2\,(g) + 2* = 2H\text{-}* \quad (7)$$

where the asterisk represents a surface site. Since the model we propose is based on the reactants, product, and intermediates chemisorbing *competitively* on a constant number of sites, it is very important to include the surface sites explicitly in the description of the reaction mechanism.

For entropy reasons the sticking coefficient for the formation of N-* from N_2 (g) is unusually small, of the order of 10^{-6} (*1, 2, 9, 11, 21, 32, 33*). The enthalpy of adsorption of N_2 (g) as N_2-* is -31.4 kJ mol^{-1} at low coverages for Fe(111) (*30*) and the activation enthalpy for dissociation of N_2-* into 2N-* is 28.1 kJ mol^{-1} (*30*), resulting in an apparent activation enthalpy for the adsorption of N_2 (g) as 2N-* of -3.3 kJ mol^{-1} (*30*) at low coverages.

The rate-limiting step in the adsorption and desorption of N_2 (sequences 1, 2) and in the synthesis of NH_3 (sequences 1–7) is step 2 (*1, 2, 9, 11, 22*).

Quantum mechanical considerations (*12, 13, 19, 21*) show that the effect of K is mostly of electrostatic origin. The dipole of K-* interacts attractively with the N_2-* dipole, increasing the synthesis rate by increasing the stability of N_2-* on the surface and thus increasing the lifetime of N_2-*. This interpretation is supported by recent EELS studies of N_2-* on Fe(111) and

K/Fe(111) (*47, 52*), and by kinetic calculations (*46*).

4. FORMULATION OF THE MODEL

Our model (*28, 29, 46*) is based on the statistical mechanical description of reactants, intermediates, and products chemisorbing competitively on identical surface sites. A number of simplyfing assumptions are introduced to ensure that the results of the model can be readily interpreted on a microscopic and macroscopic scale. The approximations of practical significance are the assumptions that the gas phase is ideal and that all sites are identical. The consequences of assuming that the gas phase is ideal can be estimated. Calculations show that the errors introduced by this approximation are tolerable under the reaction conditions considered below.

The consequences of assuming that all sites are ideal are much harder to estimate. From quantum mechanical calculations the assumption of identical sites appears obvious (*13*). The agreement between calculated (*28*) and experimental TPD peak shapes suggests that this approximation is quite good.

Based on the results of quantum mechanical calculations (*13, 21*) and the experimental study of N_2/Fe(100) (*31, 32*), adsorbate–adsorbate interactions are assumed to be absent until the coverage reaches one adsorbate atom per two Fe atoms; above this coverage repulsive adsorbate–adsorbate interactions are assumed to cause a rapid drop in the enthalpy of adsorption, thus limiting the maximum coverage to one adsorbate atom per two Fe atoms.

Using a statistical mechanical description (*28, 29, 46*) we obtain expressions for the equilibrium constants in terms of partition functions for the intermediates, e.g., for step (2)

$$K_2 = \frac{Z_{N*}^2}{Z_{N_2*}}, \tag{8}$$

where the partition function is calculated as

$$Z_X = (\Pi Z_{\text{trans},i})(\Pi Z_{\text{vib},i})(\Pi Z_{\text{rot},i}) \exp\left(-\frac{E_X}{RT}\right), \tag{9}$$

where Z_{trans}, Z_{vib}, and Z_{rot} are the partition functions for translational, vibrational, and rotational degrees of freedom for species X. E_X, the ground state energy, is of electronic origin. Translational, vibrational, and rotational degrees of freedom give the largest contributions to the entropy of species X, while E_X gives the largest contribution to the standard enthalpy of formation for this species X.

In the model the reaction steps (1) and (3)–(7) are treated as equilibria,

$$K_1 (P_{N_2}/p_0)\Theta_* = \Theta_{N_2*} \tag{10}$$

$$K_3\Theta_{N*}\Theta_{H*} = \Theta_{NH*}\Theta_* \tag{11}$$

$$K_4\Theta_{NH*}\Theta_{H*} = \Theta_{NH_2*}\Theta_* \tag{12}$$

$$K_5\Theta_{NH_2*}\Theta_{H*} = \Theta_{NH_3*}\Theta_* \tag{13}$$

$$K_6\Theta_{NH_3*} = p_{NH_3}/p_0\Theta_* \tag{14}$$

$$K_7 (p_{H_2}/p_0)(\Theta_*)^2 = (\Theta_{N*})^2 \tag{15}$$

where p_0 is the thermodynamic reference pressure, taken as 101.325 kPa.

The gas-phase equilibrium constant for the synthesis of ammonia $N_2 + 3H_2 = 2NH_3$ is

$$K_g = K_1K_2^2K_3^2K_4^2K_5^2K_6^2K_7^3. \tag{16}$$

Since a site must be either unoccupied or occupied by one of the reaction intermediates, we have

$$\Theta_{N_2*} + \Theta_{N*} + \Theta_{NH*} + \Theta_{NH_2*} + \Theta_{NH_3*} + \Theta_{H*} + \Theta_* = 1, \tag{17}$$

where Θ_* represents the fraction of sites not covered by any surface intermediate, loosely speaking, the "coverage by free sites."

For step (2) the rate is

$$r_2 = k_2\Theta_{N_2*}\Theta_* - k_{-2}(\Theta_{N*})^2. \tag{18}$$

For k_2 we use an Arrhenius expression

$$k_2 = A_2\exp(-\Delta H_2^{\ddagger}/RT). \tag{19}$$

5.1. Application to N_2 Adsorption and Desorption

We first apply the model to the adsorption and desorption of N_2. This is done by considering the nitrogen adsorption steps (steps (1), (2))

$$N_2\,(g) + * = N_2\text{-}* \quad (1)$$

$$N_2\text{-}* + * = 2N\text{-}* \quad (2)$$

which are a part of the reaction mechanism for the synthesis of ammonia (steps (1)–(7)). The equilibrium and rate equations (Eqs. (10)–(15) and (18) reduce to

$$K_1(P_{N_2}/p_0)\Theta_* = \Theta_{N_2*} \quad (10)$$

$$r_2 = k_2\Theta_{N_2*}\Theta_* - k_2/K_2(\Theta_{N*})^2. \quad (18)$$

Equation (17) reduces to

$$\Theta_{N_2*} + \Theta_{N*} = 1. \quad (20)$$

N-* will be formed at the rate $2r_2$ from which we obtain

$$\frac{d\Theta_{N*}}{dt} = \frac{2k_2K_1p_{N_2}/p_0(1 - \Theta_{N*})^2}{1 + K_1p_{N_2}/p_0} - \frac{2k_2}{K_2}(\Theta_{N*})^2. \quad (21)$$

We define the sticking coefficient, σ, and the initial sticking coefficient, σ_0, as the probability that a nitrogen molecule will form 2N-* when it hits any site or a free site, respectively. In our model, σ and σ_0 are related by

$$\sigma = \sigma_0\Theta_*^2 \quad (22)$$

and σ_0 may be calculated from

$$\sigma_0 = \frac{k_2K_1d}{p_0(1 + K_1p_{N_2}/p_0)}\sqrt{2\pi mRT}, \quad (23)$$

where d is the density of sites (mol m^{-2}) and m is the molecular mass of N_2 (0.028 kg mol^{-1}).

The activation enthalpy for σ (and σ_0) is

$$\Delta H_\sigma^\ddagger = RT^2\left(\frac{d\ln(\sigma)}{dT}\right)_p = \Delta H_2^\ddagger + \Delta H_1 + 0.5RT - \Delta H_1\Theta_{N_2*}. \quad (24)$$

5.2. Application to NH_3 Synthesis

For the synthesis of ammonia the following equations are obtained from Eqs. (10)–(15) and (17) by straightforward algebra,

$$\Theta_{N_2*} = K_1\frac{p_{N_2}}{p_0}\Theta_* \quad (25)$$

$$\Theta_{N*} = \frac{p_{NH_3}p_0^{0.5}}{K_3K_4K_5K_6K_7^{1.5}p_{H_2}^{1.5}}\Theta_* \quad (26)$$

$$\Theta_{NH*} = \frac{p_{NH_3}}{K_4K_5K_6p_{H_2}}\Theta_* \quad (27)$$

$$\Theta_{NH_2*} = \frac{p_{NH_3}}{K_5K_6K_7^{0.5}p_{H_2}^{0.5}p_0^{0.5}}\Theta_* \quad (28)$$

$$\Theta_{NH_3*} = \frac{p_{NH_3}}{K_6p_0}\Theta_* \quad (29)$$

$$\Theta_{H*} = K_7^{0.5}\frac{p_{H_2}^{0.5}}{p_0^{0.5}}\Theta_* \quad (30)$$

$$\Theta_* = \left(1 + K_1\frac{p_{N_2}}{p_0} + \frac{p_{NH_3}p_0^{0.5}}{K_3K_4K_5K_6K_7^{1.5}p_{H_2}^{1.5}} + \frac{p_{NH_3}}{K_4K_5K_6K_7p_{H_2}} + \frac{p_{NH_3}}{K_5K_6K_7^{0.5}p_{H_2}^{0.5}p_0^{0.5}} + \frac{p_{NH_3}}{K_6} + K_7^{0.5}\frac{p_{H_2}^{0.5}}{p_0^{0.5}}\right)^{-1}. \quad (31)$$

The turnover frequency for the synthesis of ammonia is found by substituting (25), (26), and (31) into (18),

$$r_2 = 2k_2K_1\left(\frac{p_{N_2}}{p_0} - \frac{p_{NH_3}^2p_0}{K_gp_{H_2}^3}\right)(\Theta_*)^2. \quad (32)$$

Each surface site will form NH_3 at a net rate of $2r_2$ NH_3 molecules per second.

6. DETERMINATION OF INPUT PARAMETERS

The thermodynamic data for N_2, H_2, and NH_3 in the gas phase are taken from standard tables (*53*). Vibrational frequencies for the adsorbed species are taken from electron energy loss spectra (*3*, *54*).

The parallel frustrated translation is treated by assuming a sinusoidally varying potential with a barrier for surface diffusion equal to 0.05 eV for N_2-* and 0.5 eV for the

other reaction intermediates. This choice of parameters is not at all critical for the final result.

Using the above information on the TPD spectra of H-* (*33*) and NH_3-* (*34*) the adiabatic ground-state energy for these species is calculated from the measured equilibrium pressure for N_2-* (*30*).

The measured initial sticking coefficient for N_2 into 2N-* and its activation enthalpy may then be used to determine A_2 and $\Delta H_2^{\ddagger}$. We use values (*35*) of the initial sticking coefficient for N_2 on K-precovered Fe to represent the industrial catalyst. Since the presence of K erases the difference in sticking coefficient for N_2 on the low-index planes of Fe (*33, 35*), no assumption is necessary on the distribution of sites between the low-index planes in the catalyst.

The ground-state energy for N-* is then found from TPD spectra (*56*). We find it important to treat the rate of adsorption and desorption of nitrogen (Eqs. (1), (2)) and the synthesis of ammonia (Eqs. (1)–(7)) by one consistent model (*57*). The ground-state energies for NH-* and NH_2-* are not available from experiments. We assign values to these two ground-state energies between the values for N-* and NH_3-*.

For the active area of the catalyst we use the area determined from CO chemisorption (*58–60*).

At this point we may examine the sensitivity of the predictions made by the model to the choice of input parameters. If the parameters are determined by the procedure outlined above, the model will correctly reproduce the gas-phase thermodynamics, the experimental thermodynamics for the adsorption of N_2-*, N-*, NH_3-*, and H-*, the experimental value for the initial sticking coefficient for N_2 into 2N-*, and its activation enthalpy. Apart from the gas-phase thermodynamics and the size of the active area only three parameters are found to be critical for the predictions by the model. The critical parameters are A_2, $\Delta H_2^{\ddagger} + E_{N_2*}$, and E_{N*}, all of which are determined rather directly from experiments.

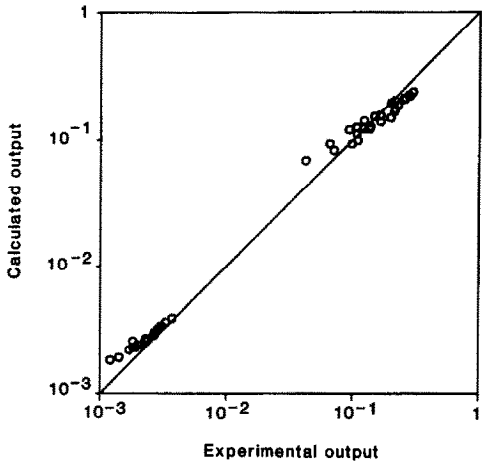

FIG. 1. Comparison of calculated and measured NH_3 mole fractions at the reactor outlet for the industrial catalyst Topsøe KM1R. The catalyst is operating at 1–300 atm, 375–500°C. The measurements at 150–300 atm are taken from Table I in Ref. (*26*). The 1-atm measurements are from Ref. (*65*).

For all other parameters, the sensitivity of the calculated results to reasonable variations of the input parameters is small. For example, changing the frequency of the frustrated translation by a factor of 10 or changing the ground-state energy for NH-* or NH_2-* by 30 kJ mol^{-1} will result in changes in the predicted rates of reaction of less than 10% (*29*).

7. COMPARISON WITH EXPERIMENT

Since all parameters in the model have been determined without reference to data measured for the synthesis of ammonia, the quality of the predictions of the model may be examined by comparing experimental and calculated data for the high-pressure synthesis of ammonia using the industrial catalyst. The data are compared in Fig. 1. The deviation between experimental and calculated data under any set of reaction conditions amounts to less than a factor of 1.4 in the rate constants for ammonia synthesis.

The good agreement between calculated and experimental output from the reactor at 1–300 atm strongly suggests that the model correctly reproduces the essential features

of the kinetics and mechanism of ammonia synthesis. This gives confidence that the model may be used to analyze the physical and chemical conditions on the surface of the catalyst during ammonia synthesis.

For the working catalyst the surface coverages by the reaction intermediates may be calculated from Eqs. (25)–(31). A typical case is shown in Fig. 2. The calculated coverages are high under all experimentally feasible conditions for ammonia synthesis. Since the formation of N-* from N_2-* is the rate-limiting step, the intermediates N-*, NH-*, NH_2-*, NH_3-*, and H-* are formed through equilibrium with H_2 and NH_3. Under conditions of vanishing $P_{NH_3}:P_{H_2}$ ratio the coverage by H-* is high, while under all other conditions, N-* is the most abundant reaction intermediate.

Since the synthesis rate may be expressed as the product of the experimental sticking coefficient σ_0 and the coverage by free sites, θ_*,

$$r_2 = \frac{\sigma_0 p_0 (1 + K_1 p_N/p_0)}{d\sqrt{2\pi m RT}} \left(\frac{p_{N_2}}{p_0} - \frac{p_{NH_3}^2 p_0}{K_g p_{H_2}^3}\right)(\Theta_*)^2. \quad (33)$$

From this equation it is apparent why the critical parameters are A_2, $\Delta H_2 + E_{N_2*}$ and $E_{N*} \cdot A_2$ and $\Delta H_2 + E_{N_2*}$ are the preexponential factor and the activation enthalpy of σ_0, K_1 is much too small to have any significance in the $1 + K_1 P_{N_2}/P_0$ term, and E_{N*} is by far the most important parameter in the calculation of θ_* since N-* is the most abundant reaction intermediate. The three critical parameters have been determined rather directly from the measured sticking coefficient and thermal desorption spectrum for N_2. The good agreement between the calculated and the experimental rates of NH_3 synthesis is thus not at all a lucky accident.

Even if N-* is by far the most abundant reaction intermediate under typical reaction conditions, the sum of the coverages by NH-*, NH_2-*, NH_3-*, and H-* is larger than the "coverage" by free sites. The kinetics cannot be well described by a

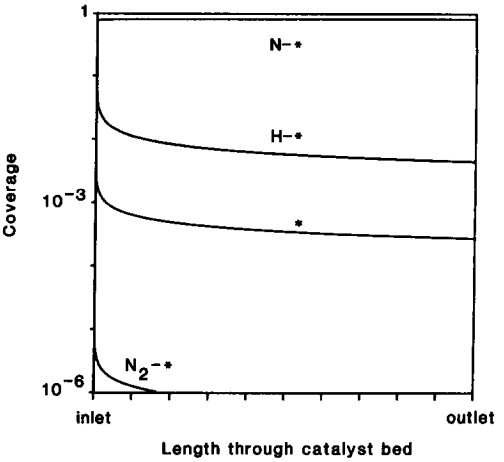

FIG. 2. Calculated coverages of adsorbed molecular nitrogen (N_2-*), chemisorbed atomic nitrogen (N-*), chemisorbed atomic hydrogen (H-*), and "coverage by free sites" (*) for a K-promoted Fe catalyst operating at 400°C, 100 atm. Inlet 25% N_2, 75% H_2, 0% NH_3; outlet 20.6% NH_3.

Langmuir–Hinshelwood expression with only one surface intermediate (*48, 50, 51, 61*). We suggest that it is the complexity arising from $\Theta_{NH*} + \Theta_{NH_2*} + \Theta_{NH_3*} + \Theta_{H*} > \Theta_*$ rather than adsorbate–adsorbate interactions or surface heterogeneity (*48, 50, 51, 61*) which is the cause of the complicated kinetics (*48, 51, 61*) deduced from early studies of ammonia synthesis.

A change in the rate-determining step at very low conversions has been suggested by Temkin *et al.* (*63*). By reanalyzing their experimental data we find (*29*) that our model adequately describes the experimental observations and that the failure of the conventional kinetics (*63*) is caused by a high coverage by H-* rather than by a change in the rate-limiting step.

8. INTERPRETATION OF REACTION ORDERS

When one considers a kinetic expression using apparent reaction orders

$$r = k\left(\frac{p_{N_2}}{p_0}\right)^{\alpha_{N_2}}\left(\frac{p_{H_2}}{p_0}\right)^{\alpha_{H_2}}\left(\frac{p_{NH_3}}{p_0}\right)^{\alpha_{NH_3}} - \frac{k}{K_g}\left(\frac{p_{N_2}}{p_0}\right)^{-1+\alpha_{N_2}}\left(\frac{p_{H_2}}{p_0}\right)^{-3+\alpha_{H_2}}\left(\frac{p_{NH_3}}{p_0}\right)^{2+\alpha_{NH_3}} \quad (34)$$

the reaction orders can be calculated from the forward rate of NH_3 synthesis (*32*),

$$r_+ = 2k_2K_1\frac{p_{N_2}}{p_0}\Theta_*^2. \quad (35)$$

The results are

$$\alpha_{N_2} = \frac{d\ln(r_+)}{d\ln(p_{N_2}/p_0)} = 1 - 2\Theta_{N_2*} \quad (36)$$

$$\alpha_{H_2} = \frac{d\ln(r_+)}{d\ln(p_{H_2}/p_0)} = 3\Theta_{N*} + 2\Theta_{NH*} + \Theta_{NH_2*} - \Theta_{H*} \quad (37)$$

$$\alpha_{NH_3} = \frac{d\ln(r_+)}{d\ln(p_{NH_3}/p_0)} = -2\Theta_{N*} - 2\Theta_{NH*} - 2\Theta_{NH_2*} - 2\Theta_{NH_3*}. \quad (38)$$

The reaction orders may thus be interpreted in terms of the surface coverages. The reaction orders are not constants but depend on the reaction conditions, as the coverages depend on the reaction conditions. Under all experimentally feasible conditions the reaction order for N_2 is predicted to be unity. Under conditions of vanishing partial pressure of ammonia, the coverage by H-* is high and we predict $\alpha_{H_2} \sim 3$, $\alpha_{NH_3} \sim 0$. Under typical ammonia synthesis conditions the reaction orders are almost, but not completely, independent of the reaction conditions. The calculated values are $\alpha_{H_2} = 3$, $\alpha_{NH_3} = -2$ in agreement with the experimental determination by Nielsen *et al.* (*49*).

At small conversions we predict that the reaction will become inhibited by H_2 and zeroth order in NH_3. Inhibition of ammonia synthesis by H_2 at small conversions has recently been reported for supported Ru (*64*).

These fractional and almost constant reaction orders found under typical conditions for ammonia synthesis are in our model obtained for identical surface sites in the absence of adsorbate–adsorbate interactions.

It should be noted that even if the reaction orders may be calculated from a knowledge of the surface coverages, the converse is not true.

The reaction orders may be calculated similarly to Eqs. (17)–(20) for other commonly used kinetic expressions for ammonia synthesis (*29*).

9. INTERPRETATION OF THE ACTIVATION ENTHALPY

The activation enthalpy for ammonia synthesis may be calculated from

$$\Delta H^\ddagger = RT^2\left(\frac{d\ln(r_+)}{dT}\right)_p. \quad (39)$$

By application of this to the rate expression (Eqs. (25)–(32)) the following equation is obtained,

$$\Delta H^\ddagger = \Delta H_2^\ddagger + \Delta H_1 - 2\Delta H_1\Theta_{N_2*} - 2(\Delta H_3 + \Delta H_4 + \Delta H_5 + \Delta H_6 + 1.5\Delta H_7)\Theta_{N*} - 2(\Delta H_4 + \Delta H_5 + \Delta H_6 + 1.0\Delta H_7)\Theta_{NH*} - 2(\Delta H_5 + \Delta H_6 + 0.5\Delta H_7)\Theta_{NH_2*} - 2\Delta H_6\Theta_{NH_3*} - \Delta H_7\Theta_{H*}. \quad (40)$$

The terms in Eq. (40) may be interpreted as the activation enthalpy for the rate-limiting step plus a weighted average of the desorption enthalpies of the reaction intermediates.

Reaction		Enthalpy
N_2-*	$= N_2$ (g) + *	$-\Delta H_1$
N-* + $1.5H_2$	$= NH_3$ + *	$-(\Delta H_3 + \Delta H_4 + \Delta H_5 + \Delta H_6 + 1.5\Delta H_7)$
NH-* + $1.0H_2$	$= NH_3$ + *	$-(\Delta H_4 + \Delta H_5 + \Delta H_6 + 1.0\Delta H_7)$
NH_2-* + $0.5H_2$	$= NH_3$ + *	$-(\Delta H_5 + \Delta H_6 + 0.5\Delta H_7)$
NH_3-*	$= NH_3$ + *	$-\Delta H_6$
H-*	$= 0.5H_2$ + *	$-0.5\Delta H_7$. (41)

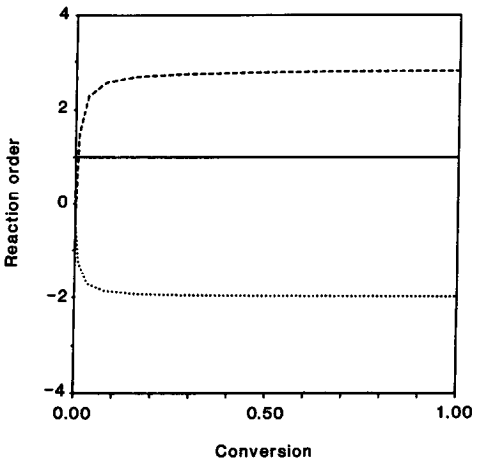

FIG. 3. Calculated reaction orders for N_2 (solid curve), H_2 (dashed curve), and NH_3 (dotted curve) for NH_3 synthesis over K-promoted Fe at 100 atm, 400°C, N : H ratio 1 : 3. Conversion defined as the ratio of the actual ammonia partial pressure to the ammonia partial pressure at thermodynamic equilibrium.

The activation enthalpy is not constant but depends on the reaction conditions (Fig. 4) as the surface coverages depend on the reactions conditions (Fig. 2). Also the reaction enthalpies depend somewhat on the reaction temperature. Under typical synthesis conditions the activation enthalpy is almost, but not completely, constant. For the experimental conditions of Nielsen *et al.* we calculate an activation enthalpy equal to 47 kJ mol^{-1} in good agreement with the experimental value equal to 46 kJ mol^{-1}.

At extremely small conversions Θ_{N*}, Θ_{NH*}, Θ_{NH_2*}, and Θ_{NH_3*} are vanishing. Under these conditions the term $-\Delta H_7\Theta_{H*}$ may become significant. We predict that at vanishing partial pressure of NH_3 and at high pressures of H_2, values of $\Delta H^{\ddagger}$ up to about 90 kJ mol^{-1} may be observed. The value of 81 kJ mol^{-1} reported for NH_3 synthesis over Fe single crystals (*22, 23*) is identical to the value predicted from our model under the same reaction conditions. The high value of $\Delta H^{\ddagger}$ in the experiment is caused by H-* rather than N-* being the most abundant surface species.

Since the activation enthalpy $\Delta H_1 + \Delta H_2^{\ddagger} = -3.3$ kJ mol^{-1} (*30*) for the rate-limiting step (Eq. (2)) is vanishing, the major contribution to the activation enthalpy for ammonia synthesis comes from chemisorption enthalpies for the intermediates. This contribution may be interpreted as the energetic cost of creating two additional free sites.

10. CONCLUSIONS

Based on the picture of ammonia synthesis emerging from the experimental study of single crystals under ultrahigh vacuum and from the theoretical investigations in chemisorption and catalysis, we have formulated a physically simple microscopic model (*28*). All parameters in the model have been determined from gas-phase thermodynamics, single-crystal studies, and an estimate of the size of the active area for the industrial catalyst. No reference to measurements of catalytic reaction rates is used in the determination of the input parameters. The model adequately reproduces the experimental reaction rates over large intervals of experimental conditions for the industrial catalyst.

The agreement between experimental high-pressure rates of ammonia synthesis

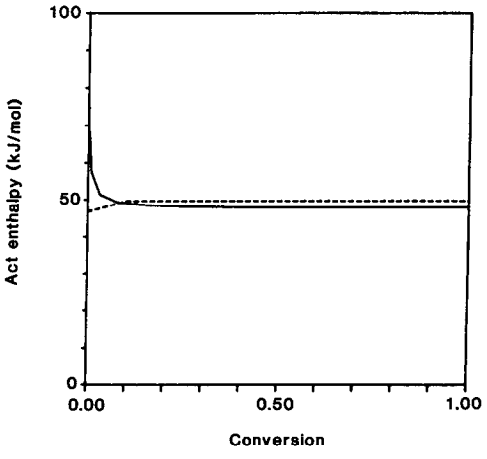

FIG. 4. Calculated activation enthalpy for ammonia synthesis over K-promoted Fe at 100 atm (solid curve) and at 1 atm (dashed curve), 400°C, N_2 : H_2 ratio 1 : 3.

and the calculations using our model strongly suggests that the detailed picture of ammonia synthesis emerging from single-crystal studies of chemisorption under UHV is correct and emphasizes the relevance and potential of single-crystal studies in catalysis research.

Further, the agreement between experiment and calclation suggests that a number of featues, such as surface recontruction and solubility of gases in bulk Fe, are of minor importance for the kinetics of NH_3 synthesis over Fe.

The description of the state of the surface of the working catalyst emerging from the calculations shows the simultaneous presence of several adsorbed species with only a few vacant sites.

The apparent reaction orders calculated from our model at 1–300 atm are in agreement with experimental determinations. The reaction orders depend on the reaction conditions but are almost constant under typical operating conditions.

The calculations show that the fractional reaction orders observed experimentally are obtained directly from reported UHV studies using a surface consisting of identical sites. The surface heterogeneity assumed in the usual derivation of the Temkin–Pyzhev kinetics (*50, 51, 61, 62*) is not observed experimentally for single crystals and our calculations show that the existence of surface heterogeneity for catalysts is unnecessary for the derivation of the observed high-pressure kinetics.

We show that the activation enthalpy of ammonia synthesis equals the sum of the activation enthalpy for the rate-limiting step plus an averaged energetic cost of creating two additional free sites on the surface. The first contribution is vanishing compared to the second.

In the model the activation enthalpy is not constant; however, the largest variations in activation enthalpy are predicted to be observable under conditions of vanishing partial pressure of ammonia. For typical high-pressure conditions the calculated activation enthalpy is in agreement with experimental determinations.

REFERENCES

1. Ertl, G., "Critical Reviews in Solid State and Materials Science," p. 349. CRC Press, Boca Raton, 1982.
2. Grunze, M., *in* "The Chemistry and Physics of Solid Surfaces and Heterogeneous Catalysis" (D. A. King and D. P. Woodruff, Eds.), Vol. 4, p. 413. Elsevier, Amsterdam, 1982.
3. Grunze, M., Golze, M., Hirschwald, W., Freund, H.-J., Pulm, H., Seip, H., Kuppers, J., and Ertl, G., *Phys. Rev. Lett.* **53,** 850 (1984).
4. Goodman, D. W., *Acc. Chem. Res.* **17,** 194 (1984).
5. Lee, M. B., Yang, Q. Y., Tang, S. L., and Ceyer, S. T., *J. Chem. Phys.* **85,** 1693 (1986).
6. Campbell, C. T., and Daube, K. A., *J. Catal.* **104,** 109 (1987).
7. Gellman, A. J., Farias, M. H., and Somorjai, G. A., *J. Catal.* **88,** 546 (1984).
8. Goodman, D. W., Kelley, R. D., Madey, T. E., and Yates, J. Y., *J. Catal.* **63,** 226 (1980).
9. Ertl, G., *in* "Catalysis, Science and Technology" (J. R. Anderson and M. Boudart, Eds.), Vol. 4, p. 208. Springer-Verlag, Berlin, 1983.
10. Campbell, C. T., *J. Catal.* **99,** 28 (1986).
11. Ertl, G., *Catal. Rev. Sci. Eng.* **21,** 201 (1980).
12. Holloway, S., Lundquist, B. I., and Nørskov, J. K., "Proceedings, 8th International Congress on Catalysis, Berlin, 1984," Vol. IV, p. 85. Verlag Chemie, Weinheim, 1984.
13. Nørskov, J. K., Holloway, S., and Lang, N. D., *Surf. Sci.* **157,** 65 (1984).
14. Feibelmann, P., and Hamann, D., *Phys. Rev. Lett.* **52,** 61 (1984).
15. Nørskov, J. K., *J. Vac. Sci. Technol.* **18,** 420 (1981).
16. Sparnaay, M. J., *Surf. Sci. Rep.* **4,** 101 (1985).
17. Upton, T. H., and Goddard, W. A., III, *Phys. Rev. Lett.* **42,** 472 (1979).
18. Umrigar, C., and Wilkins, J. W., *Phys. Rev. Lett.* **54,** 1551 (1985).
19. Lang, N. D., Holloway, S., and Nørskov, J. K., *Surf. Sci.* **150,** 24 (1985).
20. Tomanek, D., and Bennemann, K. H., *Phys. Rev. B.* **31,** 2488 (1985).
21. Nørskov, J. K., *Physica B* **127,** 193 (1984).
22. Spencer, N. D., Schoonmaker, R. C., and Somorjai, G. A., *J. Catal.* **74,** 129 (1982).
23. Spencer, N. D., Schoonmaker, R. C., and Somorjai, G. A., *Nature (London)* **294,** 1643 (1981).
24. Madix, R. J., *Adv. Catal.* **29,** 1 (1980).
25. Oh, S. K., Fisher, G. B., Carpenter, J. E., and Goodman, D. W., *J. Catal.* **100,** 360 (1986).
26. Boudart, M., and Löffler, D. G., *J. Phys. Chem.* **88,** 5763 (1984).

27. Bowker, M., Parker, I. B., and Waugh, K. C., *Appl. Catal.* **14,** 101 (1985).
28. Stoltze, P., and Nørskov, J. K., *Phys. Rev. Lett.* **55,** 2502 (1985).
29. Stoltze, P., *Phys. Scr.* **36,** 824 (1987).
30. Grunze, M., Golze, M., Fuhler, J., Neumann, M., and Schwartz, E., "Proceedings, 8th International Congress on Catalysis, Berlin, 1984," Vol. IV, p. 133. Verlag Chemie, Weinheim, 1984.
31. Ertl, G., Grunze, M., and Weiss, M., *J. Vac. Sci. Technol.* **13,** 314 (1976).
32. Boszo, F., Ertl, G., Grunze, M., and Weiss, M., *J. Catal.* **49,** 18 (1977).
33. Boszo, F., Ertl, G., Grunze, M., and Weiss, M., *Appl. Surf. Sci.* **1,** 103 (1977).
34. Weiss, M., Ertl, G., and Nietsche, F., *Appl. Surf. Sci.* **2,** 614 (1979).
35. Ertl, G., Lee, S. B., and Weiss, M., *Surf. Sci.* **114,** 527 (1982).
36. Nielsen, A., *Catal. Rev. Sci. Eng.* **23,** 17 (1981).
37. Ozaki, A., and Aika, K., *in* "Catalysis, Science and Technology" (J. R. Anderson and M. Boudart, Eds.), Vol. 1, p. 89. Springer-Verlag, Berlin, 1981.
38. Nielsen, A., "An Investigation of Promoted Iron Catalysts for the Synthesis of Ammonia." Gjellerup, Copenhagen, 1968.
39. Pennoch, G. M., Flower, H. M., and Andrew, S. P. S., *J. Catal.* **103,** 1 (1987).
40. Clausen, B. S., Mørup, S., Topsøe, H., Candia, R., Jensen, E. J., and Baranski, A., *J. Phys. (Paris) Colloq.* **37,** C6-245 (1976).
41. Solbakken, V., Solbakken, A., and Emmett, P. H., *J. Catal.* **15,** 90 (1969).
42. Ertl, G., Prigge, D., Schloegl, R., and Weiss, M., *J. Catal.* **79,** 359 (1983).
43. Silverman, D. G., and Boudart, M., *J. Catal.* **77,** 208 (1982).
44. Borghard, W. S., and Boudart, M., *J. Catal.* **80,** 194 (1983).
45. Peters, C. L., Schäfer, K., and Krabetz, R., *Z. Electrochem.* **64,** 1194 (1960).
46. Stoltze, P., and Nørskov, J. K., *J. Vac. Sci. Technol. A* **5,** 581 (1987).
47. Whitman, L. J., Bartosch, C. E., Ho, W., Strasser, G., and Grunze, M., *Phys. Rev. Lett.* **56,** 1984 (1986).
48. Boudart, M., *Catal. Rev. Sci. Eng.* **23,** 84 (1981).
49. Nielsen, A., Kjær, J., and Hansen, B., *J. Catal.* **3,** 68 (1964).
50. Boudart, M., Djega-Mariadassou, G., "Kinetics of Heterogeneous Catalytic Reactions." Princeton Univ. Press, Princeton, 1984.
51. Ozaki, A., Taylor, H., and Boudart, M., *Proc. R. Soc. London Ser. A* **258,** 47 (1960).
52. Whitman, L. J., Bartosch, C. E., and Ho, W., *J. Chem. Phys.* **85,** 3688 (1986).
53. Stuhl, D. R., and Prophet, H. (Eds.), "JANAF Thermochemical Tables," 2nd. ed. National Bureau of Standards, 1971.
54. Erley, W., and Ibach, H., *J. Electron Spectrosc. Relat. Phenom.* **31,** 61 (1983).
55. Ertl, G., Weiss, M., and Lee, S. B., *Chem. Phys. Lett.* **60,** 391 (1979).
56. Menzel, D., *in* "Chemistry and Physics of Solid Surfaces" (R. Vanselow and R. Howe, Eds.), Vol. 4, p. 389. Springer-Verlag, Berlin/New York, 1982.
57. Iche, C., and Nozieres, Ph., *J. Phys. (Paris)* **37,** 1313 (1976).
58. Emmett, P. H., and Brunauer, S., *J. Amer. Chem. Soc.* **57,** 35 (1935).
59. Benziger, J., and Madix, R. J., *Surf. Sci.* **94,** 119 (1980).
60. Topsøe, H., Topsøe, N., Bohlbro, H., and Dumesic, J. A., "Proceedings, 7th International Congress on Catalysis, Tokyo, 1980" (T. Seiyama and K. Tanake, Eds.), P. 247. Kodansha/Elsevier, Tokyo/Amsterdam, 1981.
61. Temkin, M. I., and Pyzev, V. M., *Zh. Fiz. Khim.* **13,** 851 (1939).
62. Brunauer, S., Love, K. S., and Keenan, R. G., *J. Amer. Chem. Soc.* **64,** 751 (1942).
63. Temkin, M. I., Morozov, N. M., and Shapatina, E. N., *Kinet. Catal.* **4,** 224 (1963).
64. Aika, K., Kumasaka, M., Oma, T., Kato, O., Matsuda, H., Watanabe, N., Yamazaki, K., Ozahi, A., and Onhishi, T., *Appl. Catal.* **28,** 57 (1986).
65. Stoltze, P., unpublished results.